

Interleukin-19 Promotes Retinal Neovascularization in a Mouse Model of Oxygen-Induced Retinopathy

Jingling Zou,^{1,2} Wei Tan,^{1,2} Bingyan Li,^{1,2} Zicong Wang,^{1,2} Yun Li,^{1,2} Jun Zeng,^{1,2} Bing Jiang,^{1,2} Shigeo Yoshida,³ and Yedi Zhou^{1,2}

¹Department of Ophthalmology, The Second Xiangya Hospital of Central South University, Changsha, China

²Hunan Clinical Research Center of Ophthalmic Disease, Changsha, China

³Department of Ophthalmology, Kurume University School of Medicine, Kurume, Japan

Correspondence: Yedi Zhou, Department of Ophthalmology, The Second Xiangya Hospital of Central South University, 139 Renmin Middle Road, Furong District, Changsha, Hunan 410011, China; zhouyedi@csu.edu.cn.

Received: February 24, 2022

Accepted: June 17, 2022

Published: July 11, 2022

Citation: Zou J, Tan W, Li B, et al. Interleukin-19 promotes retinal neovascularization in a mouse model of oxygen-induced retinopathy. *Invest Ophthalmol Vis Sci.* 2022;63(8):9. <https://doi.org/10.1167/iovs.63.8.9>

PURPOSE. Retinal neovascularization is a major cause of blindness. This study aimed to investigate the effects of IL-19 and the underlying mechanisms in a mouse model of oxygen-induced retinopathy (OIR).

METHODS. C57BL/6J wild-type mice and IL-19 knockout (KO) mice were used to establish an OIR mouse model. Bone marrow-derived macrophages (BMDMs) with or without recombinant IL-19 (rIL-19) stimulation were injected intravitreally. Reverse transcription-quantitative polymerase chain reaction was used to determine the mRNA expressions. ELISA and western blotting were performed to assess the protein levels. Immunofluorescence staining was applied to assess retinal neovascularization. Human retinal endothelial cells (HRECs) stimulated with rIL-19 were cultured to evaluate the effects on cell proliferation and migration.

RESULTS. The level of IL-19 was significantly elevated at postnatal day 17 in OIR retinas. Both the avascular areas and pathological neovascular tufts were significantly increased in rIL-19-treated OIR retinas and suppressed in IL-19 KO retinas. IL-19 KO mice suppressed expression of ARG1, VEGFA, and pSTAT3. Moreover, BMDMs stimulated by rIL-19 enhanced that expression and suppressed the expression of inducible nitric oxide synthase (iNOS). The proliferation and migration of HRECs were significantly augmented by rIL-19. In addition, intravitreal injection of BMDMs stimulated by rIL-19 enhanced retinal neovascularization.

CONCLUSIONS. These findings suggest that IL-19 enhances pathological neovascularization through a direct effect on microvascular endothelial cells and the promotion of M2 macrophage polarization. The inhibition of IL-19 may be a potential treatment for retinal neovascularization.

Keywords: retinal neovascularization, interleukin-19, M2 macrophage, microvascular endothelial cell, oxygen-induced retinopathy

Retinal neovascularization is a crucial contributor to the pathological conditions associated with visual impairment. Hypoxia is the main cause for retinal neovascularization and leads to increased secretion of a variety of cytokines, including vascular endothelial growth factor (VEGF), angiopoietin 2, and platelet-derived growth factor B.^{1,2} Diseases that follow this pathological process are referred to as ischemic retinopathies and include diabetic retinopathy, retinopathy of prematurity (ROP), and retinal vein occlusion.^{2,3} A mouse model of oxygen-induced retinopathy (OIR) is widely used to elucidate the pathogenesis involved in retinal neovascularization.^{4,5}

Macrophages are key to angiogenesis⁶ and have two functional phenotypes: (1) classically activated M1 and (2) alternatively activated M2.^{7,8} M1 macrophages aggravate inflammation, whereas M2 macrophages exert antiinflammatory and proangiogenesis effects.⁷⁻⁹ Our previous study found that M2 macrophages may promote the induction of certain

cytokines to strengthen retinal pathological neovascularization.¹⁰ Moreover, earlier studies have reported that the level of M2 macrophage marker in the vitreous was significantly higher in patients with proliferative diabetic retinopathy (PDR) than in non-diabetic controls,^{11,12} suggesting that macrophage M2 polarization plays an important role in retinal neovascularization.

As a crucial cytokine in the immune system,¹³ IL-19 is a Th2 cytokine that derives from systemic circulation and is mainly secreted by monocytes, the precursors of macrophages.¹⁴ Previous studies have demonstrated that IL-19 promotes angiogenesis in a variety of diseases, such as ischemic hindlimbs and myocardial infarction.^{15,16} We previously reported the antiangiogenic effects of IL-12, a crucial Th1 cytokine, in a mouse model of OIR.¹⁷ IL-19 reduced the level of IL-12 and promoted the expression of VEGFA in a hindlimb ischemia model,¹⁵ and the proangiogenic effects of IL-19 were signal transducer and activator of

transcription 3 (STAT3)-dependent in aortic rings.¹⁸ In addition, IL-19 reportedly enhances angiogenesis by promoting M2 macrophage polarization.^{16,18}

Based on the above, we hypothesized that IL-19 may be a key mediator in retinal neovascularization, both directly via regulation of the function of microvascular endothelial cells and indirectly by promoting M2 macrophage polarization. In the present study, we investigated the effect of IL-19 and the mechanisms underlying this effect in a mouse model of OIR.

MATERIALS AND METHODS

Mouse Model of OIR

C57BL/6J wild-type (WT) mice (Hunan SJA Laboratory Animal Company, Changsha, Hunan, China) and IL-19 knockout (KO) mice (Cyagen Biosciences, Taicang, Jiangsu, China) were used in our study. All experimental procedures were approved by the Institutional Animal Care and Use Committee of Central South University, China, and were carried out according to the ARVO Statement for the Use of Animals in Ophthalmic and Vision Research.

The establishment of the mouse model of OIR has been described previously.⁴ Briefly, on postnatal day 7 (P7) mouse pups were placed in a 75% oxygen chamber for 5 days. Pups were exposed to room air (RA) on P12. Pups from at least three litters were used for each experiment to overcome biological variability. The mothers of the OIR pups were rotated at P10. Age-matched mouse pups without hyperoxia treatment were included as controls.

Preparation of Macrophages from Mouse Bone Marrow

Male C57BL/6J mice, 6 to 8 weeks old, were dissected to isolate their femoral shafts, and bone marrow-derived macrophages (BMDMs) were obtained. Four mice were used each time to obtain BMDMs, and then the samples were divided into each group. These cells were incubated in RPMI 1640 medium with GlutaMAX supplement (Gibco, Waltham, MA, USA) mixed with 10% fetal bovine serum (FBS) and 50 ng/mL macrophage colony-stimulating factor (M-CSF) (R&D Systems, Minneapolis, MN, USA) for 5 days¹⁹ to promote the differentiation of macrophages. After this

period, the cells were stimulated with 100 ng/mL recombinant IL-19 (rIL-19; R&D Systems) for 24 hours. Other cells were cultured without rIL-19 for 24 hours as a control. Macrophage markers were assessed by using reverse-transcription quantitative polymerase chain reaction (RT-qPCR). Other cells were injected intravitreally into pups with OIR. Supernatants of macrophage with or without IL-19 stimulation and uncultured medium 24 hours after treatment with IL-19 were used in the Cell Counting Kit 8 (CCK-8) assay (Dojindo Laboratories, Kumamoto, Japan).

Culture of Human Retinal Endothelial Cells

Human retinal endothelial cells (HRECs; Cell Systems, Kirkland, WA, USA) were cultured with endothelial cell growth medium (ECGM; Shanghai QiDa Biotechnology, Shanghai, China) or CSC medium (Cell Systems) in 5% CO₂ at 37°C.

Intravitreal Injections of rIL-19 or Macrophages

After exposure to 75% oxygen for 5 days, pups at P12 were injected intravitreally (0.5 μ L/eye) with mouse rIL-19 (R&D Systems), which was diluted with PBS to 10 ng/ μ L and 100 ng/ μ L. The other eye was injected intravitreally with PBS. Other pups at P12 were injected intravitreally with IL-19-stimulated macrophages or control macrophages with 1×10^5 cells in 0.5- μ L PBS per eye. A Hamilton syringe (Hamilton Company, Reno, NV, USA) with a 33-gauge needle was used for the intravitreal injections. Mice were sacrificed, and eyeballs were enucleated and evaluated at P17.

RT-qPCR Assessment

Total RNA was extracted from retinas (both eyes of each mouse were collected as a sample) or cells using Invitrogen TRIzol reagent (Thermo Fisher Scientific, Waltham, MA, USA) according to the manufacturer's protocol. The concentration of isolated RNA was quantified using NanoVue Plus (GE Healthcare, Pittsburgh, PA, USA), and cDNA was synthesized with an Invitrogen First-Strand Synthesis System (Thermo Fisher Scientific). RT-qPCR was performed using TaqMan Gene Expression Assays (Applied Biosystems, Waltham, MA, USA) (see Fig. 1) and FastStart Universal SYBR Green Master Mix (Rox; Roche, Basel, Switzerland) (see Figs. 4, 5). The TaqMan probes for the assays used were

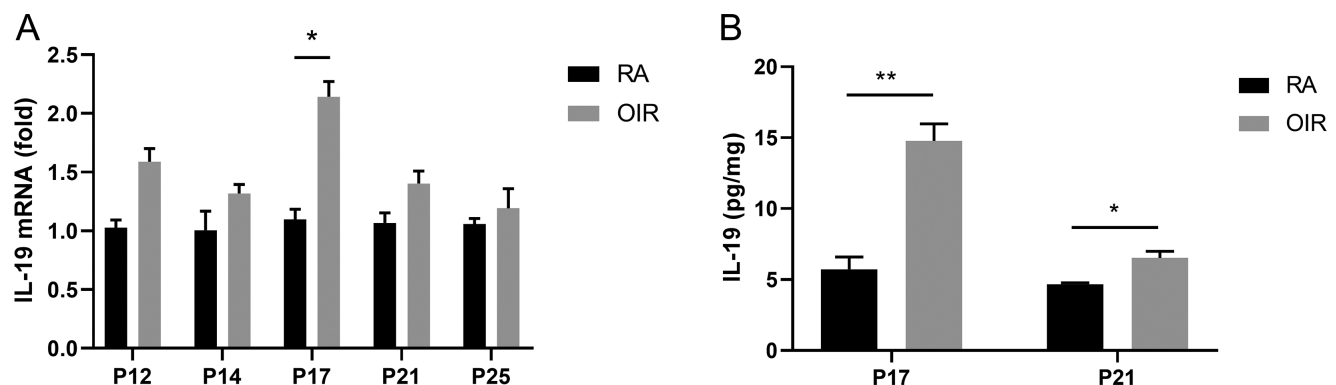


FIGURE 1. The level of IL-19 expression increases in the mouse model of OIR. (A) IL-19 mRNA levels in retinas from the OIR group reached a peak and were significantly increased compared to those in the RA group at P17. (B) The concentration of IL-19 in the OIR group was markedly increased compared with that in the RA group at both P17 and P21, and it reached a higher increase at P17. * $P < 0.05$; ** $P < 0.01$. Error bars show mean \pm SEM ($n = 4$ /group).

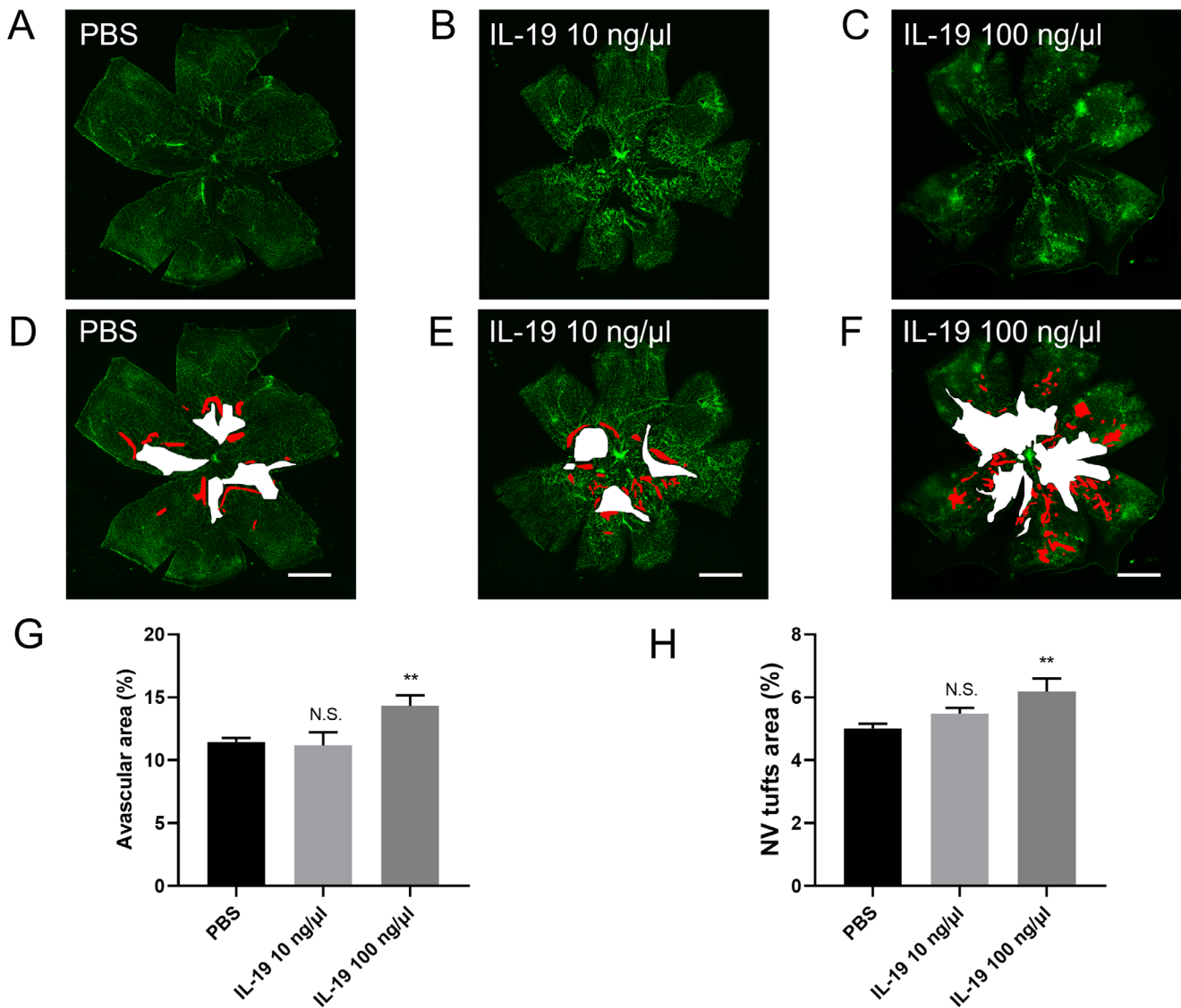


FIGURE 2. IL-19 promotes neovascularization in the retinas of the mice with OIR. The vitreous of mice with OIR were injected with 10 ng/μL or 100 ng/μL rIL-19, and the other eyes were intravitreally injected with PBS. Isolectin B4 was used to reveal the retinal vessels. Typical photographs of whole-mounted retinas demonstrate intravitreal injection of PBS (**A, D**), 10-ng/μL rIL-19 (**B, E**), and 100-ng/μL rIL-19 (**C, F**). *Red areas* represent neovascular tufts, and *white areas* represent avascular areas. There were no significant differences in the avascular areas (**G**) or neovascular tufts (**H**) between the mice injected with 10-ng/μL rIL-19 compared to the PBS control. In contrast, both the avascular areas (**G**) and neovascular tufts (**H**) were significantly larger in the mice injected with 100-ng/μL rIL-19 than in the PBS controls. ** $P < 0.01$. Error bars show mean \pm SEM ($n = 20$, $n = 10$, and $n = 10$, respectively). Scale bars: 800 μ m.

Mm99999915_g1 (glyceraldehyde 3-phosphate dehydrogenase [GAPDH]) and Mm01288324-m1 (IL-19). Gene expression levels were determined using a StepOnePlus Real-Time PCR System (Applied Biosystems). The sequences of the mouse forward and reverse primers were as follows: GAPDH (forward primer, 5'-3'-GGTGTCTCCTGCGACTTCA; reverse primer, 5'-3'-TGGTCCAGGGTTTCTTACTCC); F4/80 (forward primer, 5'-3'-TGTCTGCATGATCATCAGATA; reverse primer, 5'-3'-CGTGTCTCCTGAGTTAGAGACT); arginase 1 (ARG1; forward primer, 5'-3'-CATATCTGCCAAAGACATCGTG; reverse primer, 5'-3'-GACATCAAAGCTCAGGTGAATC); inducible nitric oxide synthase (iNOS; forward primer, 5'-3'-ACTCAGCCAAGCCCTCACCTAC; reverse primer, 5'-3'-TCCAATCTCTGCCTATCCGTCTCG); VEGFA (forward primer, 5'-3'-TAGAGTACATCTTCAAGCCGTC; reverse primer, 5'-3'-CTTCTTTGGTCTGCATTACA); IL-19 (forward primer,

5'-3'-CTCCTGGGCATGACGTTGATT; reverse primer, 5'-3'-GCATGGCTCTCTTGATCTCGT); TEK (forward primer, 5'-3'-CTAAATTTGACTTGGCAACCGA; reverse primer, 5'-3'-TCTGCTGATCACTTGTGTTTG); 3-phosphoinositide-dependent protein kinase-1 (PDK1; forward primer, 5'-3'-TTAGAGGGCTACGGGACAGATGC; reverse primer, 5'-3'-GTAATGCTTCCAGGCGGCTTTATTG). GAPDH was used to normalize the gene expression. The expression level of the genes was calculated by the $2^{-\Delta\Delta CT}$ method.

Immunofluorescence Staining

Retinas were dissected from the eyeballs as previously described,¹⁰ rinsed with PBS containing 0.1% Tween, and blocked with PBS containing 1% bovine serum albumin and 0.5% Triton X-100 (blocking buffer). The tissues were

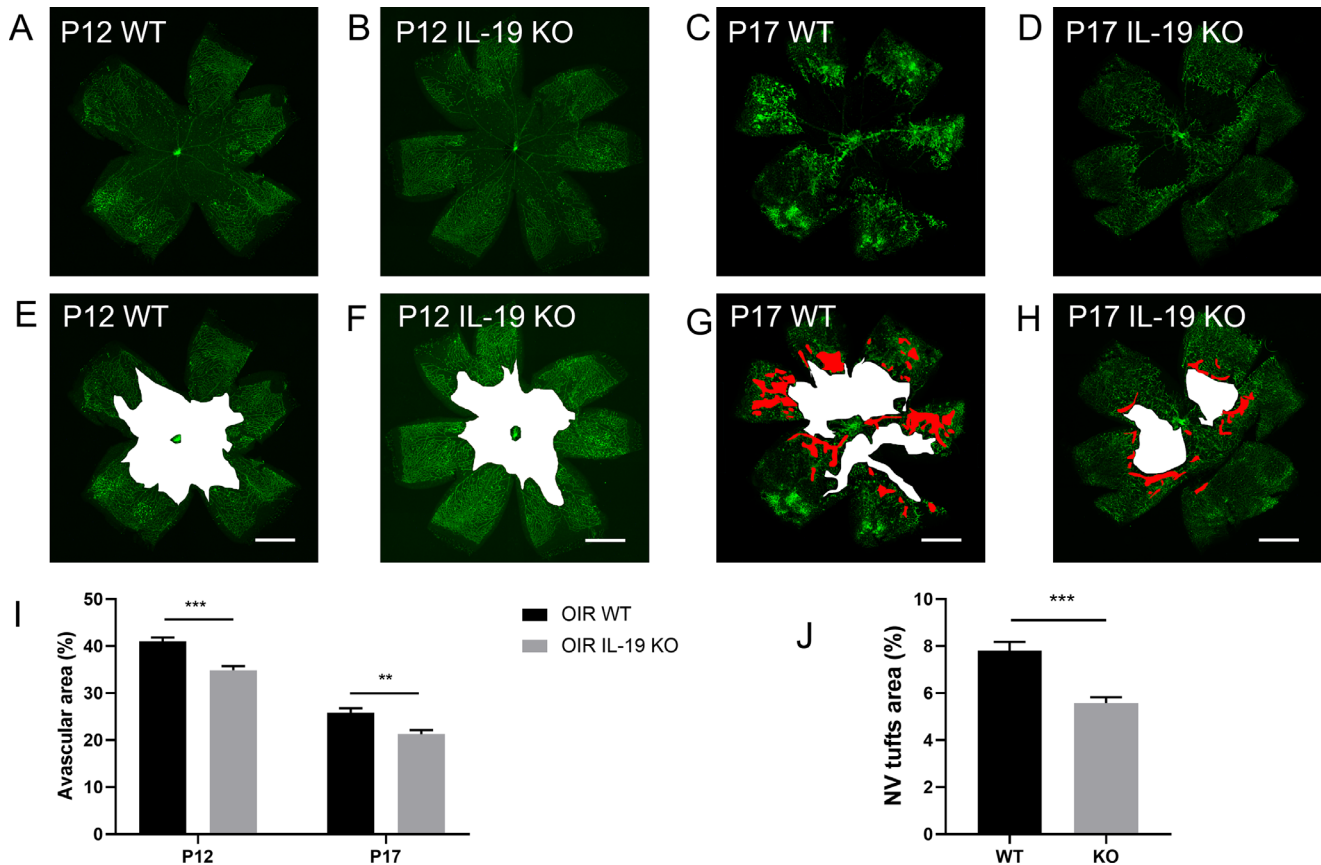


FIGURE 3. IL-19 KO suppresses neovascularization in the retinas of mice with OIR. Typical photographs of whole-mounted retinas, including WT (A, C, E, G) and IL-19 KO (B, D, F, H) retinas at P12 (A, B, E, F) and at P17 (C, D, G, H) in the mice with OIR. In the retinas with IL-19 KO, the avascular areas (I) at P12 and P17 and neovascular tufts (J) at P17 were significantly reduced compared to those of the WT control. $**P < 0.01$; $***P < 0.001$. Error bars show mean \pm SEM ($n = 12$ to 16 per group). Scale bars: 800 μ m.

then incubated in fluorescein-labeled isolectin B4 (1:150 dilution; Vector Laboratories, Burlingame, CA, USA) at 4°C overnight. After PBST (PBS containing 0.1% Tween) washes, the retinas were flatmounted on slides and covered with mounting medium (Sigma-Aldrich, St. Louis, MO, USA).

Retinal immunostaining was captured using a DMI4000B fluorescence microscope (Leica Microsystems, Wetzlar, Germany). The images were measured and analyzed using ImageJ software (National Institutes of Health, Bethesda, MD, USA) and Photoshop CS6 13.0 (Adobe Systems, San Jose, CA, USA) according to previously reported protocols.^{4,20} The avascular areas and pathological neovascular tufts were calculated as a percentage of total retinal area for each flatmount.

Measurement of IL-19 Concentration by ELISA

The retinas of the mice with OIR and RA at P17 and P21 were collected. Four samples from four pups were assayed for each group. Each sample included both retinas from a mouse. Lysis solution (USCN, Wuhan, Hubei, China) was used to extract protein from the samples. The concentration of IL-19 in retinas was assayed using an IL-19 ELISA kit (USCN) following the manufacturer's protocol.

CCK-8 Assay

HRECs were cultured with ECGM with 5% FBS and suspensions (1×10^4 cells/100 μ L) and seeded in 96-well plates. After starvation in CSC medium with 1% FBS for 8 hours, the medium was substituted with or without human rIL-19 at 10 ng/mL or 100 ng/mL (R&D Systems) or control supernatant and supernatants of macrophages treated with or without rIL-19 for 24 hours. Cell proliferation of HRECs was then determined using a CCK-8 assay (Dojindo Laboratories) according to the manufacturer's protocol.

Cell Migration Assay

HRECs were starved in CSC medium (1% FBS) for 24 hours. The lower chamber of a Transwell migration assay system with 8- μ m pores (Corning Inc., Corning, NY, USA) was coated with collagen (10 μ g/mL, 500 μ L) overnight at 4°C. After incubation and then three PBS washes, the cells (2×10^4 cells/100 μ L) were seeded into the upper chamber of the Transwell migration assay system and cultured with CSC medium (1% FBS) with or without rIL-19 at 10 ng/mL or 100 ng/mL for 24 hours. The cells were washed gently with PBS twice. The lower chamber was covered with 4% paraformaldehyde (PFA, 500 μ L) for 15 minutes and then incubated with Hoechst 33342 (1:1000 dilution, 500 μ L) for 15 minutes at room temperature. Four independent wells for

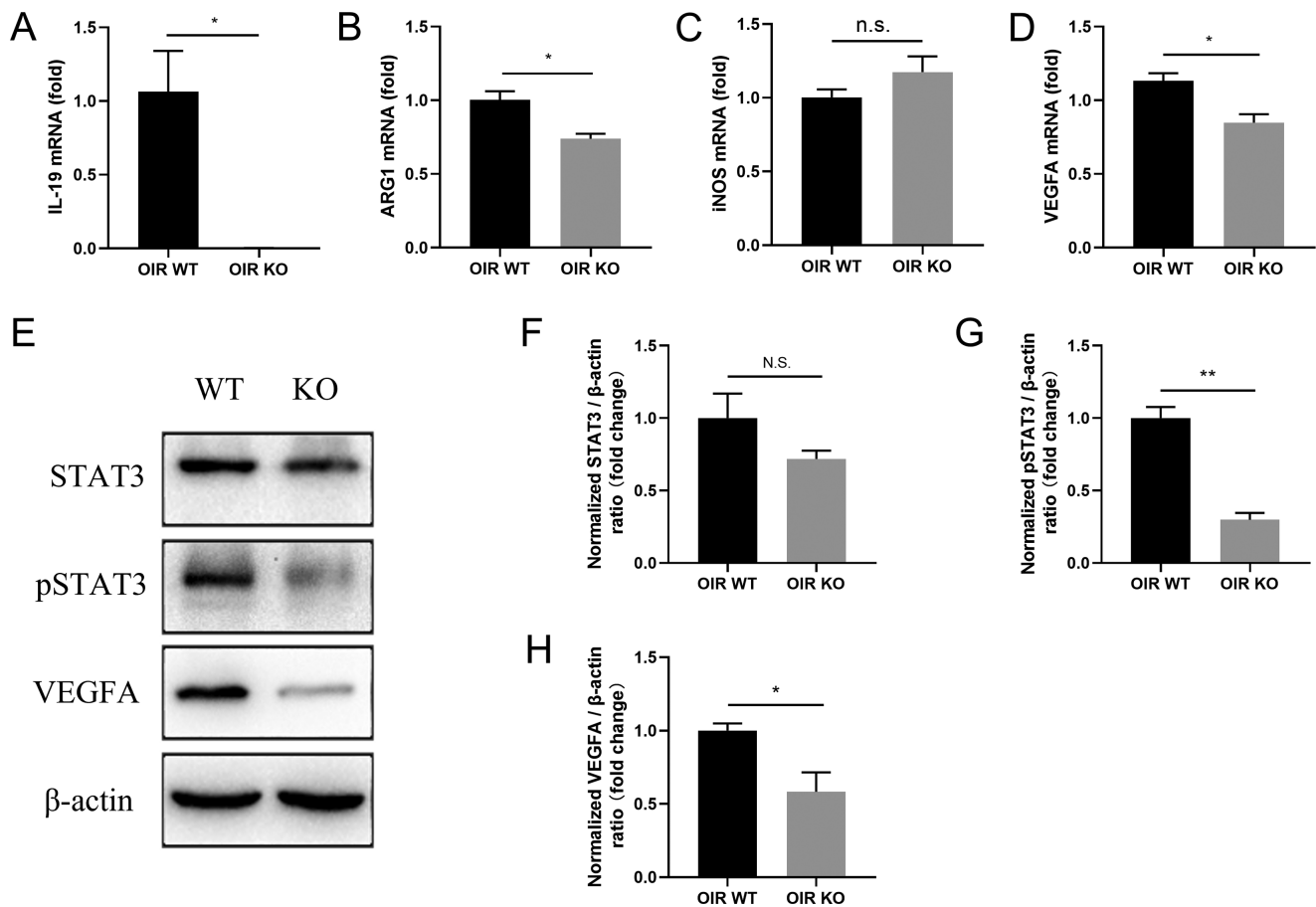


FIGURE 4. IL-19 KO mice suppress pathological neovascularization by restraining M2 polarization in retinas with OIR at P17. IL-19, ARG1 (M2 marker), iNOS (M1 marker), and VEGFA levels were detected by RT-qPCR in mice from the OIR WT and OIR IL-19 KO groups (A–D). The levels of STAT3, pSTAT3, and VEGFA proteins were examined in mice from the OIR WT and OIR IL-19 KO groups (E–H). * $P < 0.05$; ** $P < 0.01$ *** $P < 0.001$. Error bars show mean \pm SEM ($n = 3$ per group).

each group were examined, and three images per well were captured randomly.

Western Blotting

The protein of retinal tissue or bone marrow-derived monocytes was extracted using a radioimmunoprecipitation assay (RIPA) buffer and 1-mM phenylmethylsulfonyl fluoride, phosphatase inhibitors, and a protease inhibitor. The concentration of each specimen was determined using the BCA Protein Quantitation Kit (Boster Biological Technology, Wuhan, Hubei, China), and the samples were separated with SDS-PAGE and transferred to polyvinylidene difluoride filter membranes. The membranes were blocked with 5% bovine serum albumin in PBST (PBS containing 0.5% Tween) at room temperature for 1 hour and then incubated with primary antibodies overnight at 4°C. Expression of the STAT3 (1:1000 dilution; Cell Signaling Technology, Danvers, MA, USA), phospho-STAT3 (pSTAT3; 1:1000 dilution; Cell Signaling Technology), VEGFA (1:1000 dilution; Abcam, Cambridge, UK), and β -actin (1:10,000 dilution; R&D Systems) proteins in retinas with OIR at P17 and BMDMs was measured. The following day, the membranes were incubated with secondary antibodies for 1 hour at room temperature. An enhanced chemiluminescence kit (MilliporeSigma, Billerica, MA, USA) was used to detect the blots, and the bands were quantified using ImageJ software.

RNA Sequencing

RNA concentration and purity were assessed using a NanoDrop 2000 system (Thermo Fisher Scientific). The RNA 6000 Nano assay kit for the Agilent 2100 Bioanalyzer system (Agilent Technologies, Santa Clara, CA, USA) was used to measure RNA integrity. Retinas from both eyes of each mouse were collected as one sample. A total of nine samples (three each from the OIR IL-19 KO, OIR WT, and control groups) were used for RNA sequencing (RNA-seq). Equal quantities of 1- μ g RNA for each sample were used for the examination. Sequencing libraries were generated using the NEBNext Ultra RNA Library Prep Kit for Illumina (New England Biolabs, Ipswich, MA, USA) to generate sequencing libraries following the manufacturer's protocol. The raw data for the RNA-seq with the accession number GSE194176 may be searched in the Gene Expression Omnibus database (<https://www.ncbi.nlm.nih.gov/geo/>).

Gene Ontology and Kyoto Encyclopedia of Genes and Genomes Pathway Analyses

Differentially expressed genes (DEGs) were identified based on a threshold of fold change ≥ 1.5 and $P < 0.05$. Gene Ontology (GO) enrichment analysis of the DEGs was performed using the Goseq R package-based Wallenius non-central hypergeometric distribution.²¹ GO

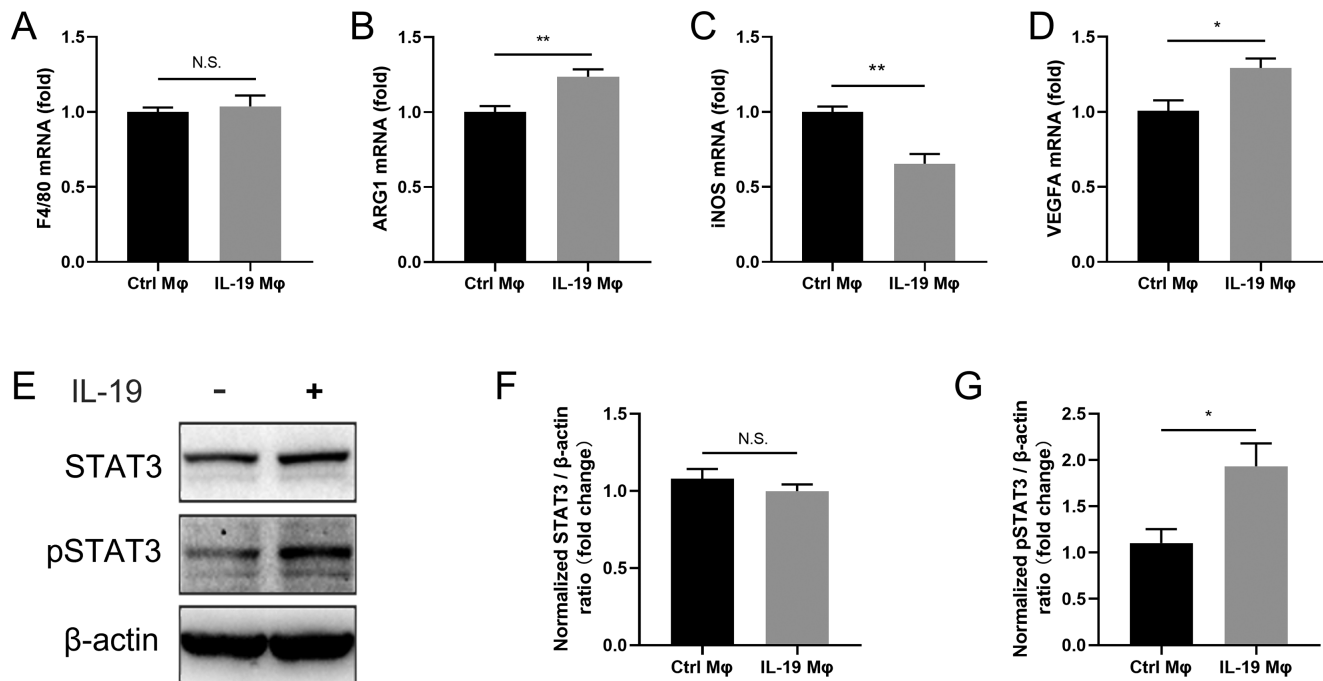


FIGURE 5. IL-19 promotes M2 polarization of BMDMs. F4/80 (A), ARG1 (B), iNOS (C), and VEGFA (D) were detected using RT-qPCR in BMDMs with or without rIL-19 stimulation ($n = 4$ per group). The protein expression of STAT3 and pSTAT3 was determined by western blotting (E–G) ($n = 3$ per group). * $P < 0.05$; ** $P < 0.01$. Error bars show mean \pm SEM.

analysis (<http://www.geneontology.org/>) and Kyoto Encyclopedia of Genes and Genomes (KEGG) pathway analysis (<http://www.genome.jp/kegg/>) were used to test the statistical enrichment of DEGs.

Statistical Analyses

Differences between two groups were assessed using Student's *t*-tests and differences among three groups were assessed by one-way ANOVA followed by Dunnett's or Tukey's multiple comparison tests. $P < 0.05$ was considered statistically significant and was determined using SPSS Statistics 19.0 (IBM, Chicago, IL, USA). All data are shown as the mean \pm standard error of the mean (SEM).

RESULTS

Upregulation of IL-19 Expression in the Mouse Model of OIR

At P17, the mRNA expression of IL-19 reached a peak and was significantly higher in the retinas with OIR than in the control retinas ($P < 0.05$) (Fig. 1A). Additionally, the ELISA results showed that the concentration of IL-19 in retinas with OIR was significantly higher than that for controls at P17 ($P < 0.01$) and P21 ($P < 0.05$) (Fig. 1B). The results suggest that IL-19 plays a crucial role during pathological neovascularization.

IL-19 Promotes Retinal Neovascularization

Five days after injection, both the avascular areas (white color) and pathological neovascular tufts (red color) were significantly increased in the retinas of the rIL-19 (100 ng/ μ L)-injected eyes compared to those of the PBS

group ($P < 0.01$) (Fig. 2). The differences in the pathological neovascular tufts (red color) and avascular areas (white color) in the mice treated with rIL-19 at a concentration of 10 ng/ μ L were not significant ($P > 0.05$). This indicates that a threshold dose of IL-19 is needed to trigger its proangiogenic effects and suggests that IL-19 had a proangiogenic function in pathological neovascularization and inhibited physiological revascularization.

Deficiency of IL-19 Suppresses Retinal Neovascularization

At P12, the retinal avascular areas (white color) in the KO mice were significantly reduced compared to those of the WT controls ($P < 0.001$) (Figs. 3A, 3B, 3E, 3F, 3I). Additionally, at P17, the IL-19 KO mice had significantly smaller pathological neovascular tufts (red color; $P < 0.001$) (Figs. 3C, 3D, 3G, 3H, 3J) and avascular areas (white color; $P < 0.01$) (Figs. 3C, 3D, 3G, 3H, 3I) than those of the WT control mice. Thus, a lack of IL-19 restricted pathological neovascularization in a mouse model of OIR.

IL-19 Deficiency Suppresses M2 Polarization and the STAT3 Pathway In Vivo

A significant decrease in the mRNA expression of IL-19 in the KO mice compared to the WT mice confirmed successful KO of the IL-19 gene ($P < 0.05$) (Fig. 4A). Compared with the WT mice, the mRNA expression of the M2 macrophage marker ARG1 ($P < 0.05$) (Fig. 4B) and VEGFA ($P < 0.05$) (Fig. 4D) was significantly decreased in the IL-19 KO mice with OIR, suggesting that IL-19 deficiency suppressed macrophage M2 polarization and restrained neovascularization. However, there was no significant difference in the mRNA expression of the M1 macrophage marker iNOS in IL-19 KO retinas and

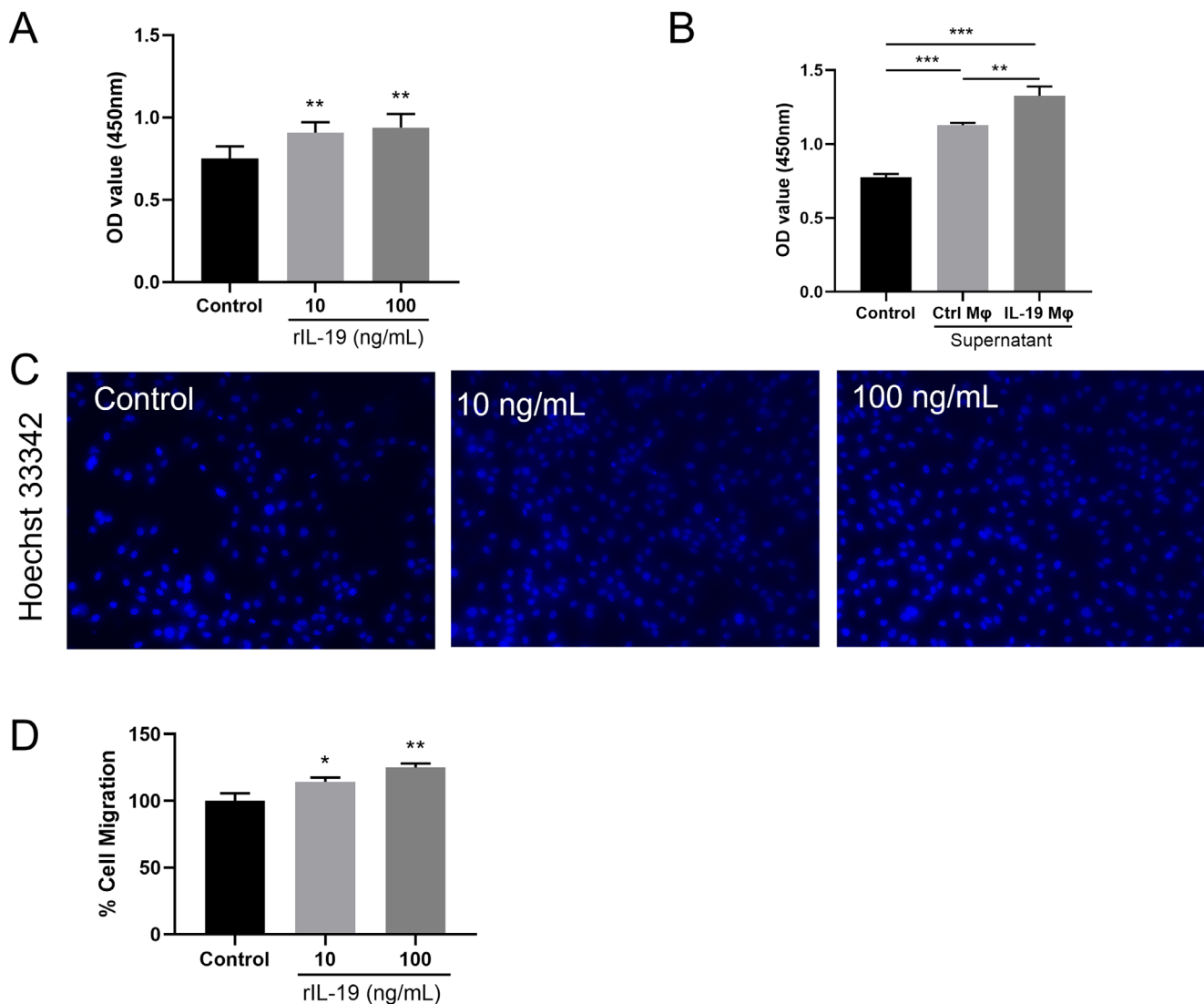


FIGURE 6. IL-19 directly and indirectly promotes the proliferation and migration of HRECs. **(A)** Treatment with either 10 ng/mL or 100 ng/mL rIL-19 for 24 hours significantly increased the optical density (OD) value of HRECs compared to that of cells without rIL-19 ($n = 6$ per group). **(B)** The supernatants of macrophages treated with or without rIL-19 for 24 hours substantially increased the OD value in comparison with that of the control cells. The supernatant of macrophages induced by rIL-19 treatment significantly increased the OD value compared with the supernatant treated without rIL-19 in HRECs ($n = 6$ per group). **(C)** The cell migration of HRECs was examined after treatment with 10 ng/mL rIL-19 and 100 ng/mL rIL-19 or without rIL-19 ($n = 4$ per group). **(D)** The groups treated with 10 ng/mL and 100 ng/mL rIL-19 both showed significantly increased cell migration compared with the group without rIL-19 treatment ($n = 4$ per group). * $P < 0.05$, ** $P < 0.01$, *** $P < 0.001$. Error bars show mean \pm SEM.

WT retinas in the OIR mouse model ($P > 0.05$) (Fig. 4C). The protein expression of VEGFA ($P < 0.05$) (Figs. 4E, 4H) was in accordance with the mRNA expression. No significant differences were found in STAT3 protein expression ($P > 0.05$) (Figs. 4E, 4F). The protein level of pSTAT3 ($P < 0.01$) (Figs. 4E, 4G) in IL-19 KO mouse retinas with OIR was significantly decreased compared to that in the WT mouse retinas with OIR.

Expression Profiles, GO Enrichment, and KEGG Pathway Analyses of DEGs

To further explore possible biological functions and pathways involved in the effect of IL-19 on retinal neovascularization, gene expressions among retinas of RA control mice,

OIR WT mice, and OIR IL-19 KO mice were measured by RNA-seq (Supplementary Fig. S1). The heat map (Supplementary Fig. S1B) indicates the top 20 genes with upregulated and downregulated expression between the OIR IL-19 KO group and the OIR WT group. A Venn diagram (Supplementary Fig. S1C) compared DEGs between the OIR WT group and the RA control group and between the OIR IL-19 KO group and the OIR WT group. The changed genes were further examined in volcano plots (Supplementary Figs. S1D, S1E).

Moreover, GO enrichment analysis and KEGG pathway analysis of DEGs were performed (Supplementary Fig. S2). KEGG pathway analysis revealed two DEGs in the hypoxia-inducible factor 1 (HIF-1) signaling pathway, TEK (also known as TIE2), and PDK1, which were common

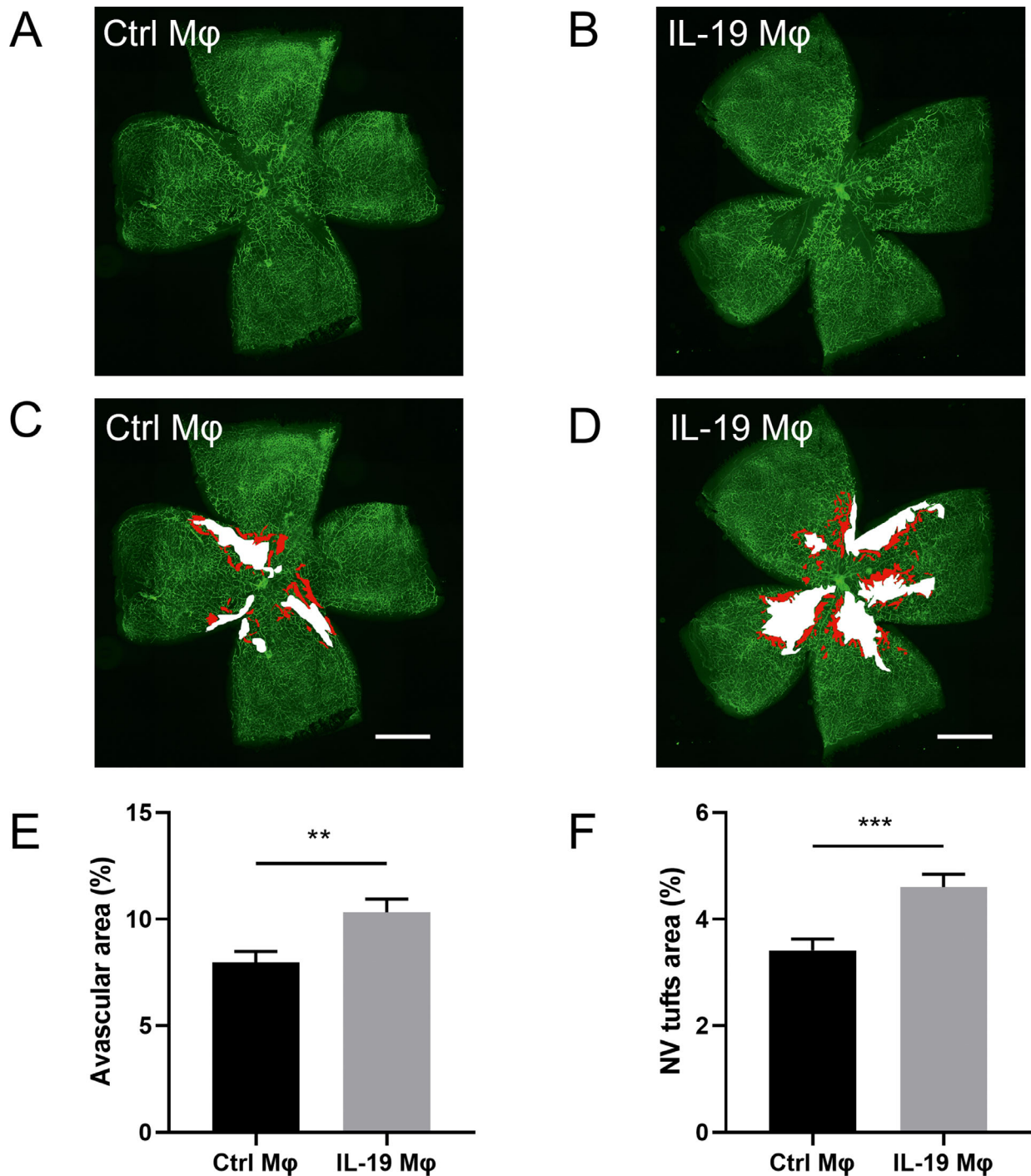


FIGURE 7. IL-19-stimulated macrophages enhance neovascularization in the retinas of mice with OIR. Typical photographs of whole-mounted retinas demonstrate intravitreal injection of bone marrow-derived control macrophages (**A, C**) and BMDMs with rIL-19 stimulation (**B, D**). The avascular areas (**E**) and neovascular tufts (**F**) were dramatically increased in the retinas injected with IL-19-stimulated macrophages compared to the control macrophages. $**P < 0.01$; $***P < 0.001$. Error bars show mean \pm SEM ($n = 14$ per group). Scale bars: 800 μ m.

to RA control and OIR WT mice, and to OIR WT and OIR IL-19 KO mice. We examined mRNA expression of them and found that TEK was significantly increased and PDK1 was significantly decreased in OIR IL-19 KO retinas compared to OIR WT retinas (Supplementary Fig. S3).

IL-19 Promotes M2 Polarization and Enhances the STAT3 Pathway in BMDMs

No significant differences were found in the mRNA expression of F4/80 (pan macrophage) between the control macrophages and the rIL-19-stimulated macrophages

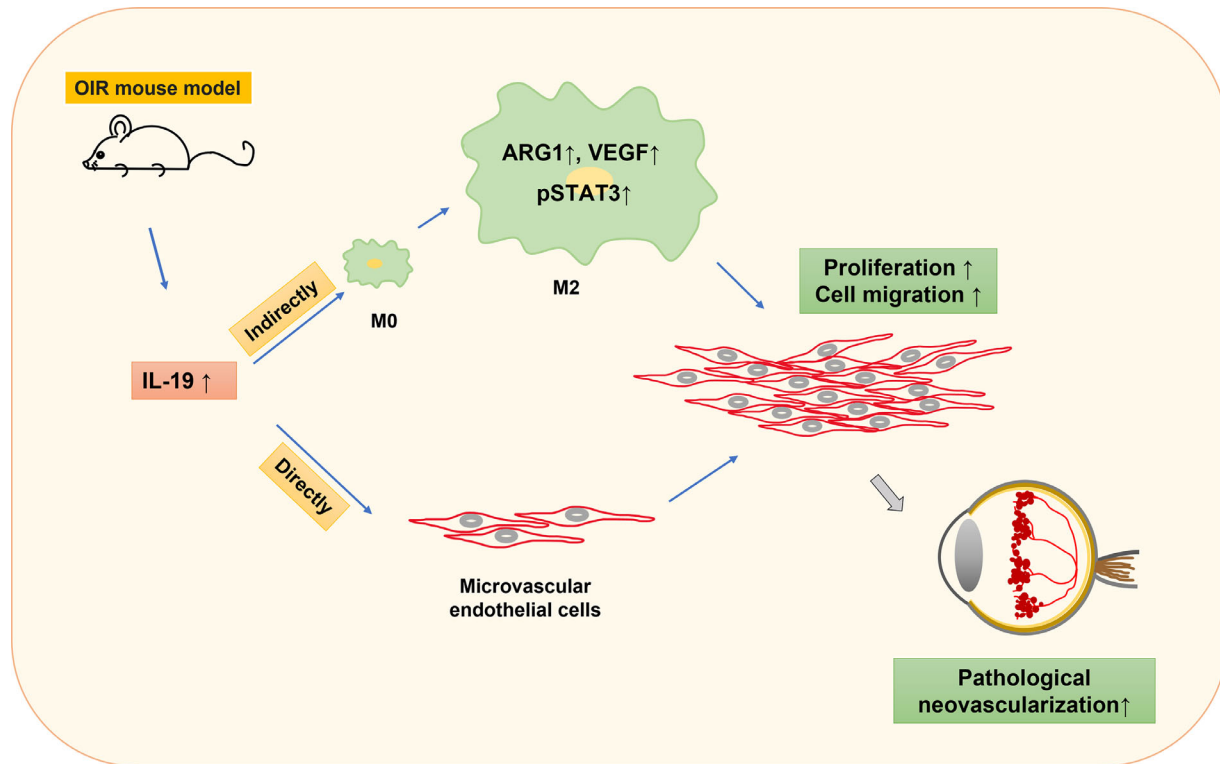


FIGURE 8. Schematic representation of the proposed proangiogenic mechanism of IL-19 in the mouse model of OIR. Increased IL-19 in the mouse model of OIR promoted pathological neovascularization both directly and indirectly. IL-19 directly enhances the proliferation and migration of microvascular endothelial cells in retinas and indirectly promotes macrophage M2 polarization. The coordination of both mechanisms caused pathological neovascularization in the mouse model of OIR.

($P > 0.05$) (Fig. 5A). The mRNA expression of ARG1 ($P < 0.01$) (Fig. 5B) was significantly increased and iNOS ($P < 0.01$) (Fig. 5C) was significantly decreased in the rIL-19-stimulated macrophages compared to the control macrophages. The mRNA expression level of VEGFA ($P < 0.05$) (Fig. 5D) was significantly increased in the rIL-19-stimulated macrophages compared with controls. The protein expression of STAT3 did not differ significantly in BMDMs with or without IL-19 stimulation ($P > 0.05$) (Figs. 5E, 5F), but the protein level of pSTAT3 in the IL-19-stimulated macrophages was significantly increased compared with that in the control macrophages ($P < 0.05$) (Figs. 5E, 5G). These findings suggest that IL-19 promotes M2 macrophage polarization and enhances the STAT3 pathway.

IL-19 Promotes Proliferation and Migration of HRECs

The CCK-8 assay demonstrated that the proliferation of HRECs was promoted by rIL-19 at either 10 ng/mL or 100 ng/mL compared with that of the control group ($P < 0.01$ and $P < 0.01$, respectively) (Fig. 6A). The percentage of cell migration was increased by human rIL-19 at both 10 ng/mL and 100 ng/mL, but the increase induced by rIL-19 at 10 ng/mL was less than that for 100 ng/mL ($P < 0.05$ for IL-19 at 10 ng/mL and $P < 0.01$ for IL-19 at 100 ng/mL) (Figs. 6C, 6D). These results indicated that IL-19 directly promotes the proliferation and migration of HRECs.

The results of the CCK-8 assay showed that the supernatants cultured both with and without rIL-19 enhanced the proliferation of HRECs compared to the control supernatants ($P < 0.001$ and $P < 0.001$, respectively) (Fig. 6B), and the supernatants cultured with rIL-19 significantly increased the number of HRECs compared to the supernatants cultured without rIL-19 ($P < 0.01$).

Bone Marrow–Derived IL-19–Stimulated Macrophages Enhance Pathological Neovascularization and Inhibit Physiological Revascularization in Retinas With OIR

At P17, both the avascular areas and pathological neovascular tufts were increased in the IL-19-stimulated macrophage-injected group compared with the control macrophage-injected group ($P < 0.01$ and $P < 0.001$, respectively) (Fig. 7). The results indicate that IL-19 exerts proangiogenic functions via macrophages in retinal neovascularization. These findings indicate that IL-19 promotes angiogenesis not only directly but also indirectly by promoting macrophage M2 polarization to mediate this effect. The proposed mechanism is shown schematically in Figure 8.

DISCUSSION

Macrophages are a crucial component of tissue homeostasis^{22–24} through mediation of tissue proliferation, angiogenesis, and metastasis.^{25–27} IL-19 contributes to angiogenesis in various diseases, including ischemic hindlimbs,¹⁵ spinal

cord injury,²⁸ and myocardial infarction.¹⁶ However, how IL-19 contributes to the development and maintenance of retinal neovascularization is poorly understood. The present study investigated the effects of IL-19 in a mouse model of OIR and in vitro angiogenesis by using HRECs to determine whether IL-19 promotes angiogenesis through M2 polarization of macrophages.

It has been reported that IL-19 expression is increased in certain inflammatory diseases, such as human leukocyte antigen B27 (HLA-B27)-associated uveitis,²⁹ inflammatory bowel disease,³⁰ and chronic rhinosinusitis.³¹ In patients with type 2 diabetes mellitus with angiopathy³² or nephropathy,³³ serum IL-19 levels were found to be higher than in control patients, and this increase was positively correlated with glycosylated hemoglobin, insulin resistance, and urinary albumin excretion rate, which indicates that IL-19 may play an important role in contributing to the progression of diabetic vasculopathy. However, there is a lack of current studies on IL-19 levels in human PDR cases. It would be interesting to further assess the expression level of IL-19 in retinal neovascular diseases such as PDR and ROP in future studies. Our results show that IL-19 mRNA and protein levels significantly increased at P17 in the retinas with OIR compared with the control retinas (Fig. 1), indicating that IL-19 probably plays a crucial role in retinal neovascularization. The peak of pathological neovascularization in an OIR mouse model occurs at P17,⁴ after which the neovascularization spontaneously regresses, consistent with changes in the level of IL-19. Therefore, the production of IL-19 may be associated with macrophages and neovascularization in OIR.

Intravitreal injection of rIL-19 at 100 ng/ μ L (0.5 μ L/eye) inhibited physiological revascularization and enhanced the pathological neovascularization (Fig. 2). However, injection of rIL-19 at 10 ng/ μ L (0.5 μ L/eye) did not significantly promote retinal neovascularization. This finding may reflect the increased IL-19 in the OIR mouse pathological condition, requiring larger amounts of IL-19 to take effect. In addition, KO of IL-19 promoted physiological revascularization and reduced pathological neovascularization at P17 (Fig. 3). These results indicate that IL-19 probably plays a crucial role in regulating pathological neovascularization and physiological revascularization.

In a mouse model of myocardial infarction and ischemic hindlimbs, IL-19 promoted polarization toward M2 macrophages and inhibited proinflammatory M1 macrophage polarization.^{15,16} After treatment with IL-19 in mice with spinal cord injury, mRNA levels of the M1 macrophage marker iNOS or CD86 decreased significantly, and those of the M2 macrophage markers ARG1, YM1, and CD206 substantially increased.^{16,28} In addition, ARG1, YM1, and Krüppel-like factor 4 (KLF4) levels in spleen tissue of IL-19^{-/-} mice are significantly lower than in WT mice.¹⁵ Our findings are consistent with those of earlier studies and demonstrate that significantly less ARG1 is expressed in retinas of mice with IL-19 deficiency than in WT mice in the OIR mouse model (Fig. 4). In bone marrow-derived macrophages, IL-19 treatment also induced the M2 phenotype in macrophages.^{15,34} In our study, the rIL-19-stimulated macrophages showed increased expression of ARG1 and decreased expression of iNOS compared to the macrophages without rIL-19 in vitro (Fig. 5), consistent with former studies. However, the difference between mRNA expression of iNOS in IL-19 KO retinas and WT retinas in the OIR mouse model was not significant, which may be because

macrophages comprise only a small percentage of retinal cells so that the iNOS difference in these retinas is negligible. Both in vivo and in vitro studies have indicated that IL-19 promotes angiogenesis by enhancing M2 macrophage polarization in retinal neovascularization.

VEGF is a key player in angiogenesis that mediates endothelial cell signaling by binding to VEGF receptor 2 (VEGFR2).^{35,36} Accumulating evidence has revealed that IL-19 accelerates angiogenesis by upregulating VEGF expression in both model mice^{16,18,28} and BMDMs.¹⁵ In the present study, the KO of IL-19 reduced both mRNA and protein expression of VEGFA in the retinas of OIR mice (Fig. 4), suggesting that IL-19 deficiency may be a potential therapeutic strategy to prevent pathological neovascularization. However, VEGFA in the retina is produced by many types of cells, including macrophages, Müller glia, HRECs and retinal pigment epithelial cells.³⁷⁻³⁹ Therefore, reduced VEGFA in the KO retina may be due not only to macrophage polarization but also to changes in the variety of cells, thus requiring further investigation in future studies.

Previous studies have indicated that IL-19 induces the activation of STAT3.^{16,18,34} One study showed that angiogenic activity of IL-19 in aortic rings is STAT3 dependent,¹⁸ and another demonstrated that IL-19 signals activate STAT3 through the IL-19 receptor and the IL-20Ra and IL-20Rb receptor complex in myeloid cells.⁴⁰ In our study, IL-19 KO significantly reduced the levels of VEGFA and pSTAT3 (Fig. 4). Additionally, rIL-19-stimulated macrophages showed significantly enhanced protein expression of pSTAT3 compared to those without rIL-19 in vitro. These results suggest that the proangiogenic effects resulted from IL-19 through mechanisms dependent on VEGFA and activation of the STAT3 signaling pathway.

In the current study, we found that IL-19 enhanced migration of HRECs (Fig. 6), indicating a direct proangiogenic function of IL-19 on HRECs in culture. Furthermore, we observed robust induction of pathological neovascularization in retinas injected intravitreally with IL-19-stimulated macrophages compared with control macrophages (Fig. 7). These observations demonstrate that IL-19 has not only direct effects but also indirect effects by promoting macrophages to enhance angiogenesis.

The results of RNA-seq showed that the expression of HIF-1 α was not significantly different between OIR WT mice and OIR IL-19 KO mice. However, two DEGs, TEK and PDK1, were found in the HIF-1 signaling pathway according to the KEGG pathway analysis and validated by RT-qPCR (Supplementary Fig. S3). TEK is a tyrosine kinase receptor that mediates the activity of angiopoietins.⁴¹ PDK1, an ancient serine-threonine kinase, plays a crucial role in angiogenesis.⁴²⁻⁴⁴ This indicates that the reduction of VEGFA in the KO retina was not due to direct inhibition of HIF-1 α expression but was probably achieved by regulating activation of the HIF-1 signaling pathway, the exact mechanism of which requires further research. In addition, KEGG pathway analysis of the DEGs revealed several important pathways between the OIR WT group and the OIR IL-19 KO group, including cell-adhesion molecules (CAMs), the HIF-1 signaling pathway, the Toll-like receptor signaling pathway, and other signaling pathways (Supplementary Fig. S2D), which deserve to be further studied.

In conclusion, IL-19 enhances pathological retinal neovascularization both directly through microvascular endothelial cells and indirectly by promoting M2 macrophage polarization in a mouse model of OIR. There-

fore, the inhibition of IL-19 may be regarded as a potential treatment option for retinal neovascular diseases.

Acknowledgments

Supported by grants from the National Natural Science Foundation of China (81800855); Scientific Research Project of Hunan Provincial Health Commission (202207022574); Hunan Provincial Science and Technology Department (2020SK2086); Hunan Provincial Innovation Foundation for Postgraduate (CX20210115); and Fundamental Research Funds for the Central Universities of Central South University (2021zzts0358).

Disclosure: **J. Zou**, None; **W. Tan**, None; **B. Li**, None; **Z. Wang**, None; **Y. Li**, None; **J. Zeng**, None; **B. Jiang**, None; **S. Yoshida**, None; **Y. Zhou**, None

References

- Usui-Ouchi A, Aguilar E, Murinello S, Friedlander M. An allosteric peptide inhibitor of HIF-1 α regulates hypoxia-induced retinal neovascularization. *Proc Natl Acad Sci USA*. 2020;117:28297–28306.
- Campochiaro PA. Molecular pathogenesis of retinal and choroidal vascular diseases. *Prog Retin Eye Res*. 2015;49:67–81.
- Chen JF, Zhang S, Zhou R, et al. Adenosine receptors and caffeine in retinopathy of prematurity. *Mol Aspects Med*. 2017;55:118–125.
- Connor KM, Krah NM, Dennison RJ, et al. Quantification of oxygen-induced retinopathy in the mouse: a model of vessel loss, vessel regrowth and pathological angiogenesis. *Nat Protoc*. 2009;4:1565–1573.
- Hombrebueno JR, Lynch A, Byrne EM, et al. Hyaloid vasculature as a major source of STAT3(+) (signal transducer and activator of transcription 3) myeloid cells for pathogenic retinal neovascularization in oxygen-induced retinopathy. *Arterioscler Thromb Vasc Biol*. 2020;40:e367–e379.
- Polverini PJ. Role of the macrophage in angiogenesis-dependent diseases. *EXS*. 1997;79:11–28.
- Sica A, Erreni M, Allavena P, Porta C. Macrophage polarization in pathology. *Cell Mol Life Sci*. 2015;72:4111–4126.
- Orecchioni M, Ghosheh Y, Pramod AB, Ley K. Macrophage polarization: different gene signatures in M1(LPS+) vs. classically and M2(LPS-) vs. alternatively activated macrophages. *Front Immunol*. 2019;10:1084.
- Mantovani A, Sica A, Sozzani S, Allavena P, Vecchi A, Locati M. The chemokine system in diverse forms of macrophage activation and polarization. *Trends Immunol*. 2004;25:677–686.
- Zhou Y, Yoshida S, Nakao S, et al. M2 macrophages enhance pathological neovascularization in the mouse model of oxygen-induced retinopathy. *Invest Ophthalmol Vis Sci*. 2015;56:4767–4777.
- Kobayashi Y, Yoshida S, Nakama T, et al. Overexpression of CD163 in vitreous and fibrovascular membranes of patients with proliferative diabetic retinopathy: possible involvement of periostin. *Br J Ophthalmol*. 2015;99:451–456.
- Abu El-Asrar AM, Ahmad A, Allegaert E, et al. Interleukin-11 overexpression and M2 macrophage density are associated with angiogenic activity in proliferative diabetic retinopathy. *Ocul Immunol Inflamm*. 2020;28:575–588.
- Rutz S, Wang X, Ouyang W. The IL-20 subfamily of cytokines—from host defence to tissue homeostasis. *Nat Rev Immunol*. 2014;14:783–795.
- Gallagher G, Dickensheets H, Eskdale J, et al. Cloning, expression and initial characterization of interleukin-19 (IL-19), a novel homologue of human interleukin-10 (IL-10). *Genes Immun*. 2000;1:442–450.
- Richards J, Gabunia K, Kelemen SE, Kako F, Choi ET, Autieri MV. Interleukin-19 increases angiogenesis in ischemic hind limbs by direct effects on both endothelial cells and macrophage polarization. *J Mol Cell Cardiol*. 2015;79:21–31.
- An W, Yu Y, Zhang Y, Zhang Z, Yu Y, Zhao X. Exogenous IL-19 attenuates acute ischaemic injury and improves survival in male mice with myocardial infarction. *Br J Pharmacol*. 2019;176:699–710.
- Zhou Y, Yoshida S, Kubo Y, et al. Interleukin-12 inhibits pathological neovascularization in mouse model of oxygen-induced retinopathy. *Sci Rep*. 2016;6:28140.
- Kako F, Gabunia K, Ray M, et al. Interleukin-19 induces angiogenesis in the absence of hypoxia by direct and indirect immune mechanisms. *Am J Physiol Cell Physiol*. 2016;310:C931–C941.
- Manzanero S. Generation of mouse bone marrow-derived macrophages. *Methods Mol Biol*. 2012;844:177–181.
- Ishikawa K, Yoshida S, Nakao S, et al. Bone marrow-derived monocyte lineage cells recruited by MIP-1 β promote physiological revascularization in mouse model of oxygen-induced retinopathy. *Lab Invest*. 2012;92:91–101.
- Young MD, Wakefield MJ, Smyth GK, Oshlack A. Gene ontology analysis for RNA-seq: accounting for selection bias. *Genome Biol*. 2010;11:R14.
- Lavine KJ, Pinto AR, Epelman S, et al. The macrophage in cardiac homeostasis and disease: JACC Macrophage in CVD Series (Part 4). *J Am Coll Cardiol*. 2018;72:2213–2230.
- Guilliams M, Thierry GR, Bonnardel J, Bajenoff M, et al. Establishment and maintenance of the macrophage niche. *Immunity*. 2020;52:434–451.
- Brestoff JR, Wilen CB, Moley JR, et al. Intercellular mitochondria transfer to macrophages regulates white adipose tissue homeostasis and is impaired in obesity. *Cell Metab*. 2021;33:270–282.e8.
- DeNardo DG, Ruffell B. Macrophages as regulators of tumour immunity and immunotherapy. *Nat Rev Immunol*. 2019;19:369–382.
- Xu F, Cui WQ, Wei Y, et al. Astragaloside IV inhibits lung cancer progression and metastasis by modulating macrophage polarization through AMPK signaling. *J Exp Clin Cancer Res*. 2018;37:207.
- Cui X, Morales RT, Qian W, et al. Hacking macrophage-associated immunosuppression for regulating glioblastoma angiogenesis. *Biomaterials*. 2018;161:164–178.
- Guo J, Wang H, Li L, Yuan Y, Shi X, Hou S. Treatment with IL-19 improves locomotor functional recovery after contusion trauma to the spinal cord. *Br J Pharmacol*. 2018;175:2611–2621.
- Abu El-Asrar AM, Berghmans N, Al-Obeidan SA, et al. Expression of interleukin (IL)-10 family cytokines in aqueous humour of patients with specific endogenous uveitic entities: elevated levels of IL-19 in human leucocyte antigen-B27-associated uveitis. *Acta Ophthalmol*. 2019;97:e780–e784.
- Steinert A, Linas I, Kaya B, et al. The stimulation of macrophages with TLR ligands supports increased IL-19 expression in inflammatory bowel disease patients and in colitis models. *J Immunol*. 2017;199:2570–2584.
- Pace E, Scafidi V, Di Bona D, et al. Increased expression of IL-19 in the epithelium of patients with chronic rhinosinusitis and nasal polyps. *Allergy*. 2012;67:878–886.
- Li L, Y ZH-Q, Juan-Yu H, et al. Association between interleukin-19 and angiotensin-2 with vascular complications in type 2 diabetes. *J Diabetes Investig*. 2016;7:895–900.
- Li L, Jiang XG, Hu JY, et al. The association between interleukin-19 concentration and diabetic nephropathy. *BMC Nephrol*. 2017;18:65.

34. Gabunia K, Ellison S, Kelemen S, et al. IL-19 halts progression of atherosclerotic plaque, polarizes, and increases cholesterol uptake and efflux in macrophages. *Am J Pathol*. 2016;186:1361–1374.
35. Kim TK, Park CS, Jang J, et al. Inhibition of VEGF-dependent angiogenesis and tumor angiogenesis by an optimized antibody targeting CLEC14a. *Mol Oncol*. 2018;12:356–372.
36. Longchamp A, Mirabella T, Arduini A, et al. Amino acid restriction triggers angiogenesis via GCN2/ATF4 regulation of VEGF and H₂S production. *Cell*. 2018;173:117–129.e14.
37. Peach CJ, Mignone VW, Arruda MA, et al. Molecular pharmacology of VEGF-A isoforms: binding and signalling at VEGFR2. *Int J Mol Sci*. 2018;19:1264.
38. Keir LS, Firth R, Aponik L, et al. VEGF regulates local inhibitory complement proteins in the eye and kidney. *J Clin Invest*. 2017;127:199–214.
39. Wang H, Yang Z, Jiang Y, et al. Quantitative analyses of retinal vascular area and density after different methods to reduce VEGF in a rat model of retinopathy of prematurity. *Invest Ophthalmol Vis Sci*. 2014;55:737–744.
40. Gallagher G, Eskdale J, Jordan W, et al. Human interleukin-19 and its receptor: a potential role in the induction of Th2 responses. *Int Immunopharmacol*. 2004;4:615–626.
41. Akwii RG, Sajib MS, Zahra FT, Mikelis CM. Role of angiopoietin-2 in vascular physiology and pathophysiology. *Cells*. 2019;8:471.
42. Yamazaki T, Akada T, Niizeki O, Suzuki T, Miyashita H, Sato Y. Puromycin-insensitive leucyl-specific aminopeptidase (PILSAP) binds and catalyzes PDK1, allowing VEGF-stimulated activation of S6K for endothelial cell proliferation and angiogenesis. *Blood*. 2004;104:2345–2352.
43. Siu MKY, Jiang YX, Wang JJ, et al. PDK1 promotes ovarian cancer metastasis by modulating tumor-mesothelial adhesion, invasion, and angiogenesis via $\alpha 5\beta 1$ integrin and JNK/IL-8 signaling. *Oncogenesis*. 2020;9:24.
44. Miao Y, Wang W, Dong Y, et al. Hypoxia induces tumor cell growth and angiogenesis in non-small cell lung carcinoma via the Akt-PDK1-HIF1 α -YKL-40 pathway. *Transl Cancer Res*. 2020;9:2904–2918.